Characterization of a Cloned Temperature-Sensitive Construct of the Diphtheria Toxin A Domain†

Jason W. Lee, Eun Cho, Elda Aghaian, Elsa Aghaian, Joshua Der, and Bernadine J. Wisnieski*

Department of Microbiology, Immunology, and Molecular Genetics, Molecular Biology Institute, and Jonsson Comprehensive Cancer Center, University of California, Los Angeles, California 90095

Received August 5, 2004; Revised Manuscript Received November 19, 2004

ABSTRACT: Our goal was to determine how the DTM mutant construct of the A domain of diphtheria toxin (DTx) causes temperature-sensitive effects in *Drosophila* and yeast [Bellen, H. J., D'Evelyn, D., Harvey, M., Elledge, S. J. (1992) *Development 114*, 787−796]. Because DTM fortuitously bears the same point mutation as found in the A chain of CRM197, an ADP-ribosyltransferase (ADPrT)-deficient form of DTx, we hypothesized that the dramatic low-temperature-sensitive effects did not stem from ADP-ribosylation of elongation factor 2 (EF-2). To rule out acquisition of ADPrT activity at low temperatures, we assayed mutant forms of the A domain of DTx produced by in vitro transcription/translation and found that DTM has no ability to ADP-ribosylate EF-2 at 18 or 30 °C. Because the DTM gene results in a protein with a 23-amino acid missense carboxy-terminal extension, we also constructed a form without this extension. Assays for nuclease activity revealed that nuclease activity comigrated with the two distinguishable *E. coli*-cloned mutant proteins DTM and DTM-23, regardless of whether electrophoresis was conducted under denaturing or nondenaturing conditions in gels embedded with DNA. Studies with CRM197 showed that Ca^{2+} and Mg^{2+} promote single-strand DNA nicks, whereas Mn^{2+} promotes double-strand DNA breaks. Evidence that the cation-dependent nuclease and NAD-dependent ADPrT enzymic sites are distinct is that NAD protected only the A domain of DTx from proteolytic cleavage, whereas DNA protected the A domains of both DTx and CRM197. We conclude that the nuclease activity of DTM is responsible for the temperature-sensitive effects associated with its expression in both yeast and *Drosophila*.

The long-held dogma that target cell death by diphtheria toxin (DTx)[1] results solely from its ability to shut off protein synthesis was ultimately found to be incompatible with our finding that protein synthesis inhibition does not ipso facto induce cell death (*1*), a finding subsequently confirmed by others (*2*). During our in-depth investigation of DTx-induced cell death, we established that internucleosomal DNA damage preceded target cell lysis by ∼3 h (*1*). Thus, target cell death involves a process akin to apoptosis. Subsequently, we discovered that the A domain of DTx possesses a potent cation-dependent deoxyribonuclease activity (*3*, *4*). Unlike DTx's NAD-dependent ADP-ribosyltransferase (ADPrT) activity with elongation factor-2 (EF-2), an activity that requires proteolytic cleavage and reduction of the toxin and that has pH and temperature optima of 8.5 and 25 °C, respectively (*5*, *6*), DTx's nuclease activity occurs optimally under physiologically-relevant conditions (pH 7.4, 37 °C) and does not require toxin cleavage and reduction (*3*, *7*−*9*). We later established that the well-defined A domain of CRM197 also possesses nuclease activity and that this activity is 4 times greater than that of bovine pancreatic DNase I (*13*). CRM197 is a G52→E52 mutant form of DTx that lacks NAD-binding and ADP-ribosylation activities (*10*−*12*). Because there is no evidence that the A domain of CRM197 can enter the cytoplasm of cells, investigations have relied on microinjection and intracellular expression to study its behavior therein (*14*, *15*).[2]

Using a yeast mutagenesis-screening assay, Bellen et al. isolated four temperature-sensitive mutant forms of the A domain of DTx (*15*). When linked to the Drosophila *ninaE* promoter, these mutant A domains led to blindness in flies emerging from pupae incubated for 4−6 h at 16 °C. This effect was determined to be the result of apoptosis of specific photoreceptor cells, thus demonstrating the value of temperature-sensitive toxin constructs to achieving and identifying promoter-dependent cell ablation. DNA sequence analysis revealed that three of the four mutant constructs were novel: DTN, DTR, and DTI. The fourth mutant form, DTM, unexpectedly bore the same point mutation as the A domain of CRM197. Because CRM197 lacks NAD binding and ADPrT activities (*10*−*12*), even at subphysiological temperatures[2,3] and with a large excess of NAD,[2] the simplest

† This work was supported by National Institutes of Health Grant GM-22240, American Cancer Society Grants IM-716 and IM-716A, and the UCLA Academic Senate.

* Corresponding author. Telephone: (310) 206-6121. Fax: (310) 206-3865. E-mail: bwisni@microbio.ucla.edu.

[1] Abbreviations: DTx, diphtheria toxin; CRM197, the G52E mutant form of DTx; DTA, cloned A domain of wild-type DTx; DTM, cloned A domain of CRM197; DTA-23, DTA without the carboxy-terminus 23-amino acid extension; DTM-23, DTM without the carboxy-terminus 23-amino acid extension; DTN and DTR, amino- and carboxy-terminus deletion mutants of DTA, respectively; ADPrT, ADP-ribosyltransferase; EF-2, elongation factor-2; IPTG, isopropyl-*β*-D-galactopyranoside; CB, Coomassie blue; EB, ethidium bromide.

[2] A. Sodhi et al. submitted for publication.

[3] B. J. Wisnieski, personal communication (reported in ref *15*).

10.1021/bi048317p CCC: $30.25
Published on Web 01/25/2005

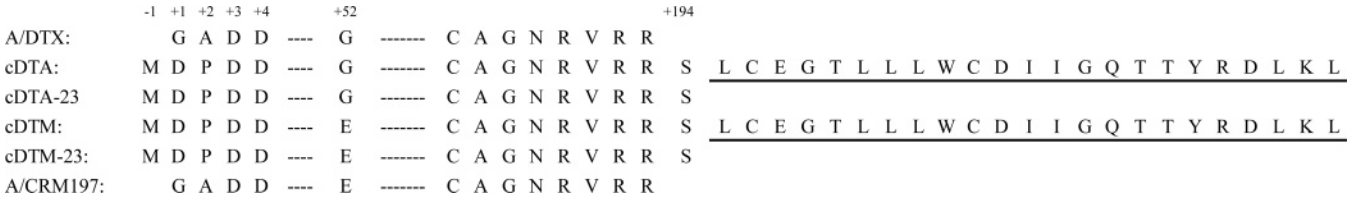

FIGURE 1: Comparison of the sequences of the proteins described in this report. Amino acids 1−193 define the mature form of the A domain of DTx (A/DTx). Serine 194 is the first amino acid of the B domain. Methionine is labeled −1 to maintain alignment between the natural and cloned (c) forms of the A domains. The "random" 23-amino acid C-terminal extension was uncovered by Bellen and coworkers (*15*).

hypothesis for DTM's cytotoxic effects in yeast and *Drosophila* (*15*) would be that it, like the A domain of CRM197, has the ability to cleave DNA. We tested this hypothesis herein with *Escherichia coli*-cloned and in vitro-translated forms and established that DTM has an intrinsic ability to bind and degrade DNA but no ability to ADP-ribosylate EF-2 at 18 or 30 °C.

These results demonstrate that apoptosis of *Drosophila* photoreceptor cells and growth inhibition in yeast stem from DTM's possession of nuclease activity and not some low-temperature-acquired ADPrT activity. This is the first demonstration of a biological role for toxin nuclease activity.

EXPERIMENTAL PROCEDURES

Reagents. Intact DTx and CRM197 were obtained from List Biological Laboratories (Campbell, CA). Intact monomeric DTx refers to DTx purified as described (*3*). Nicked DTx and CRM197 were prepared using endopeptidase argC (*3*, *13*). Prestained molecular weight markers were obtained from Bio-Rad Laboratories. TPCK-treated trypsin was obtained from Worthington. Adenylate phosphate-^{32}P-labeled-NAD was obtained from NEN Life Sciences. Lambda phage DNA was obtained from New England BioLabs, pBluescript KS$^+$ DNA from Stratagene, pUC8 DNA from Pharmacia, and *Eco*RI from Promega. Calf thymus DNA, herring testes DNA, endopeptidase argC, and NAD were obtained from Sigma. All solutions were prepared with glass-distilled deionized H_2O. Because Na^+ inhibits nuclease activity (*7*), Tris-base (Sigma) was used rather than Tris-HCl to prepare pH 7.4 Tris stocks. Plasmids pSE979-A, -M, -N, and -R were provided by Hugo J. Bellen (Howard Hughes Medical Institute, Baylor College of Medicine).

In Vitro Transcription/Translation and ADPrT Assay. DTA, DTM, DTN, and DTR genes were removed from their respective yeast plasmids (pSE979-A, -M, -N, -R) by *Kpn*1/*Xba*1 digestion and ligated into the *Kpn*1/*Xba*1 site of the pGEM-3Z expression vector (Promega, Madison, WI) under the control of the T7 promoter. The recombinant plasmids were transformed into *E. coli* JM109 and clones were screened for the correct insert by mini-plasmid preparation and restriction digestion. The pGEM-3Z plasmids containing the appropriate genes (pGEM-3Z−A, −M, −N, −R) were made on a large scale, linearized, and in vitro transcribed using T7 polymerase essentially as described (Technical Manual, Promega). The mRNAs encoding DTA, DTM, DTN, and DTR were quantified by absorbance at 260 nm and translated (0.2 μg of mRNA/10 μL of reaction) for defined times (10, 20, and 40 min) at 30 °C using a rabbit reticulocyte lysate translation system (Technical Manual, Promega). Control samples contained luciferase mRNA. All reactions were stopped with 1 μg of RNase. To determine the ADPrT activity of the translated proteins, adenylate phosphate-^{32}P-labeled NAD (30 Ci/mmol) was added (final concentration 2 μM), and the samples were incubated for 1 h at either 18 or 30 °C before electrophoresis in SDS-12.5% polyacrylamide gels (*16*). To detect ^{32}P-labeled EF-2, the gels were dried and exposed to Fuji RX film for 20 h.

Growth Conditions and Cloned-Protein Expression. Plasmids containing the genes for DTA (pET23-dA) and DTM (pET23-dM) were prepared from pGEM-3Z−A and pGEM-3Z−M, respectively, using *Nco*1 and *Hin*dIII digestion and ligation into the expression vector pET23-d. Plasmids pET23-dA, pET23-dM, pET23-dA-23, and pET23-dM-23 coded for proteins herein called DTA, DTM, DTA-23, and DTM-23, respectively (Figure 1). Plasmids pET23-dA-23 and pET23-dM-23 were prepared by polymerase chain reaction using the appropriate oligonucleotide primers. Each plasmid plus the no-toxin control plasmid (pET23-d) was transformed into the *E. coli* cell line BL21 (*Epicurian coli*; Novagen, Madison, WI). Transformed cells were cultivated in 40 mL of Luria broth (10 g of tryptone, 5 g of yeast extract, 10 g of NaCl, and 150 mg of carbenicillin per liter, pH 7.5) at 37 °C on a shaker. At the beginning of the exponential phase (∼40 Klett units), some cultures received isopropyl-β-D-galactopyranoside (IPTG; 24 μg/mL). When cells reached the plateau phase (∼200 Klett units), they were spun down and washed twice in 40 mL of Tris−saline (20 mM Tris, 150 mM saline, pH 7.4), and each pellet (∼0.5 mL) was either frozen in concentrated form or diluted with 2 mL of Tris−saline before freezing (−85 °C).

Nuclease Activity Assay in DNA-Embedded Gels. Electrophoresis under nondenaturing conditions was as follows: *E. coli* samples (25 μL each) were solubilized (5 or 10 min, 37 °C) in 1% Tergitol NP-40 and run in a 1% Tergitol NP-40−12.5% polyacrylamide gel containing herring testes DNA (20 μg/mL). The gel had a 10% stacking gel prepared with SDS-free lower gel buffer, pH 8.8 (*16*), and no DNA. It was prerun for 20 h at 10 mA. Details of nondenaturing sample preparations are as follows: *E. coli* pellets (5 μL) were resuspended in buffer (25 μL of MM#A + 20 μL of TSE, where MM#A consists of 60 μL of 10% Tergitol NP-40, 4.8 μL of 100 mM EDTA, 23.52 μL of 100% glycerol, 29.94 μL of 4× lower gel buffer without SDS (*16*), and 182.28 μL of H_2O, and TSE consists of 15 mM Tris, 150 mM NaCl, 1 mM EDTA, pH 7.4) and diluted another 10-fold with the same buffer containing 0.05% 2-mercaptoethanol. After electrophoresis, one portion of the gel was stained with Coomassie Blue (CB). The rest of the gel was incubated in 40 mM Tris, 2 mM $CaCl_2$, 2 mM $MgCl_2$, and 0.04% NaN_3 (pH 7.6) for 90 min at room temperature and then blotted with Whatman 40 filter paper, sealed between two acetate

sheets, and incubated at 30 °C for 3 h prior to ethidium bromide (EB) staining.

E. coli samples electrophoresed under denaturing conditions were solubilized (2 min, 100 °C) in SDS-reducing buffer (containing 0.05% 2-mercaptoethanol) or SDS-nonreducing buffer and run in SDS−12.5% polyacrylamide gels that contained herring testes DNA (20 μg/mL). All gels were prerun for at least 3 h. After electrophoresis, all gels were washed three times in 40 mM Tris and 0.04% NaN_3 (pH 7.6) to remove detergent and allow for protein renaturation. They were then incubated at 30 °C in 40 mM Tris, 2 mM $CaCl_2$, 2 mM $MgCl_2$, and 0.04% NaN_3 (pH 7.6) prior to EB staining. To visualize nuclease-active bands, the gels were photographed under UV light. The dark, nonfluorescent regions of the EB-stained gel represent areas of DNA degradation by underlying nuclease-active proteins. Subsequently, the gels were stained with CB for protein visualization. All gels and running buffers contained EDTA (1 mM). All methods were as previously described (*3*, *9*, *13*, *17*).

Agarose Gel Assays. Intact CRM197 (0.011 μg in 1 μL of H_2O) was equilibrated for 10 min at 22 °C with 5 μL of buffer containing 20 mM Tris, pH 7.5, and either 20 mM $MnCl_2$ or 4 mM $CaCl_2$ plus 6 mM $MgCl_2$. Reactions were initiated by adding either *Eco*RI-linearized pUC8 DNA (0.12 μg in 4 μL of H_2O) or supercoiled pBluescript KS^+ DNA (0.2 μg in 4 μL of H_2O). After specified times at 22 °C, the reactions were stopped by adding 10 μL of gel loading buffer (7.5% glycerol, 0.125% xylene cyanol, 0.125% bromophenol blue, 25 mM EDTA). Samples were held on ice before electrophoresis in 1% agarose gels containing EB (0.5 μg/mL). After a 1-h wash, gels were photographed under UV illumination.

Trypsin Protection Assays. Intact DTx (6 μg) and intact CRM197 (6 μg) were treated with trypsin (0.06 μg) for 1 h at 37 °C in the absence or presence of NAD (0.1−10 μg/40 μL) or λDNA (0.1−10 μg/40 μL). The buffer composition of each 40 μL sample was 10 mM Tris, 2 mM EDTA, pH 7.6. NAD and DNA stocks were in 10 mM Tris, 2 mM EDTA, adjusted to pH 7.6 to ensure no lowering of sample pH upon their addition. Samples without trypsin served as controls. After incubation, samples were mixed with 40 μL of reducing-denaturing buffer, boiled for 2 min, and electrophoresed in SDS−12.5% polyacrylamide gels embedded with calf thymus DNA (20 μg/mL). All gels were prerun for 2 h. Subsequently, the gels were treated for expression of nuclease activity and stained with EB. Identical 40-μL samples (the samples described above represent 40-μL portions of larger volume samples) were electrophoresed under the same conditions and then immediately stained with CB or silver for protein visualization. See above for DNA-embedded polyacrylamide gel methods.

RESULTS

Protein Sequences. With two exceptions, the protein sequence of the plasmid-encoded DTA is identical to that of the A domain of DTx, and the protein sequence of the plasmid-encoded DTM is identical to that of the A domain of the G52E mutant form of DTx called CRM197. As shown in Figure 1, there are two exceptions: (1) both amino termini are MDPDD instead of GADD, and (2) both contain a 23-amino acid missense extension at their carboxy termini. This extension arose from an inadvertent stop codon error in Maxwell and co-workers' parental DTA construct (*18*) that was not detected until the gene was fully sequenced by another group (*15*). Two other mutant constructs with temperature-sensitive effects in yeast and *Drosophila* are DTN and DTR (*15*). We have determined that DTN is missing 14 amino-terminal amino acids when compared to the plasmid-encoded DTA.[4] DTR is missing 39 carboxy-terminal amino acids plus the 23 amino acid extension (*15*).

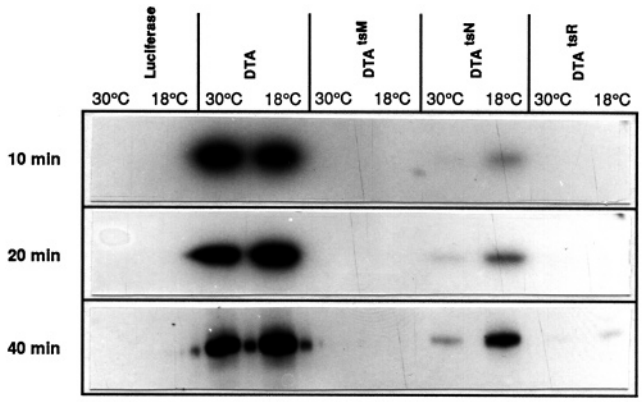

FIGURE 2: ADPrT activity of in vitro translated DTA, DTM, DTN, and DTR. The autoradiographic data shown depicts the levels of ADP-ribosylated EF-2 produced from in vitro-translated luciferase, DTA, DTM, DTN, and DTR. Translation was for 10, 20, and 40 min at 30 °C before the addition of RNase and a subsequent 1-h incubation at either 18 or 30 °C in the presence of ^{32}P-NAD. For methods, including SDS−polyacrylamide gel electrophoresis and autoradiography, see Experimental Procedures.

Detection of ADPrT Activity through Use of an in Vitro Transcription/Translation System. To characterize the ADPrT activities of in vitro-translated DTA, DTM, DTN, and DTR, we added ^{32}P-NAD and looked for ^{32}P-ADP-ribosylation of EF-2 in a rabbit reticulocyte lysate. Addition of ^{32}P-NAD results in a temperature- and mutant-dependent labeling of a 98-kDa band consistent with NAD-dependent ADP-ribosylation of EF-2. As seen in Figure 2, DTM had no detectable ADPrT activity at 18 or 30 °C, even when film exposure was increased from 20 h without an intensifying screen to 3 days with an intensifying screen. The 18 and 30 °C data for luciferase, DTA, DTN, and DTR are shown for comparison.

Use of ^{35}S-methionine (instead of ^{32}P-NAD) determined that DTA, DTN, DTM, and DTR were all synthesized to the same extent in this cell-free translation system, i.e., a system in which the endogenous NAD level is insufficient to allow for DTA inhibition of its own translation.[4] Moreover, in a yeast expression system, the level of EF-2 available for ADP-ribosylation did not change with time, regardless of whether DTM was expressed at 18 or 30 °C.[3] We conclude from these observations that DTM's temperature-sensitive cytotoxic effects in yeast and *Drosophila* are not the result of low-temperature-acquired ADPrT activity.

Expression of E. coli-Cloned DTA and DTM. Data in Figure 3 establish significant expression of DTA and DTM in *E. coli* after IPTG induction. Here, sample electrophoresis was done under reducing conditions in an SDS−polyacrylamide gel. *E. coli* bearing the gene for DTA are shown in lanes 3 (+IPTG) and 4 (−IPTG). *E. coli* bearing the gene

[4] B. J. Wisnieski et al., manuscripts in preparation.

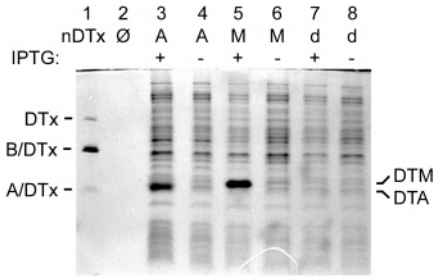

FIGURE 3: Expression of DTA and DTM in *E. coli*. Lane 1 contains 5 μg of argC-nicked DTx (nDTx). Lane 2 contains no sample. Lanes 3 and 4 contain *E. coli* that harbors DTA on the pET23-d plasmid. Lanes 5 and 6 contain *E. coli* that harbors DTM on the pET23-d plasmid. Lanes 7 and 8 contain *E. coli* that harbors the pET23-d plasmid without any *tox* gene (pET23-d, negative control). Cell samples in lanes 3, 5, and 7 were induced with IPTG. *E. coli* harboring pET23-dA, pET23-dM, and pET23-d, are designated A, M, and d, respectively. A/DTx is defined in Figure 1. B/DTx refers to the B domain of DTx. All samples were electrophoresed under reducing conditions in an SDS−polyacrylamide gel, which was then stained with CB.

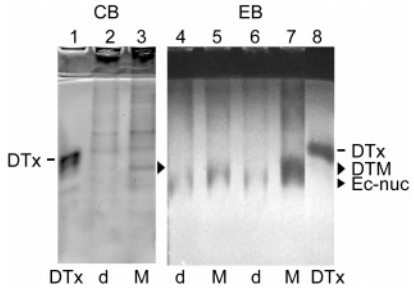

FIGURE 4: Nuclease activity of DTx and DTM after electrophoresis under nondenaturing, nonreducing conditions. Lane 1 contains of "intact" DTx (5 μg), lane 2 contains control *E. coli* (+ pET23-d), and lane 3 contains DTM-expressing *E. coli* (+ pET23-dM). Samples in lanes 1, 2, and 3 are identical to those in lanes 8, 6, and 7, respectively, except that gel lanes 1, 2, and 3 were stained with CB immediately after electrophoresis, whereas gel lanes 4−8 were treated to locate the nuclease-active bands with EB before staining with CB (Experimental Procedures). Lanes 4 and 6 contain control *E. coli* solubilized at 37 °C for 5 and 10 min, respectively; lanes 5 and 7 contain DTM-expressing *E. coli* solubilized at 37 °C for 5 and 10 min, respectively; lanes 1 and 8 contain "intact" DTx (5 μg) solubilized at 37 °C for 10 min. Solubilization was with Tergitol NP-40 under nonreducing conditions. All *E. coli* samples were induced with IPTG. The dark, nonfluorescent regions of the EB-stained gel represent areas of DNA degradation by underlying nuclease active proteins. Ec-nuc designates the position of an endogenous *E. coli* nuclease. The arrowhead between lanes 3 and 4 designates the position of the DTM protein.

for DTM are shown in lanes 5 (+IPTG) and 6 (−IPTG). *E. coli* bearing the plasmid without any toxin gene are shown in lanes 7 (+IPTG) and 8 (−IPTG). There are three arginines between the A and B domains of intact DTx. The lower two bands in lane 1 represent the B and A domains, respectively, of endoproteinase argC-nicked DTx. The top band in lane 1 is DTx that escaped cleavage by endoproteinase argC.

In this experiment, densitometric analysis revealed that the amount of DTA expression in lane 3 is ∼40% of the total *E. coli* protein and the amount of DTM expression in lane 5 is ≥50% of the total *E. coli* protein. The DTA protein (lane 3) is slightly higher in molecular weight than the A domain of the endoproteinase argC-cleaved DTx (lane 1). This is as expected, because the DTA construct bears an additional 23-amino acid carboxy-terminus extension (Figure 1). The DTM protein (lane 5) runs slightly higher than the DTA protein (lane 3) because the G52E point mutation inexplicably results in a protein that runs with a higher than expected molecular weight in SDS−polyacrylamide gels (*13*).

Western blot analysis with anti-DTx antibodies and amino acid sequencing capable of detecting any underlying protein bands at the sub-nanogram level confirmed the identities of DTA and DTM and revealed low levels of DTA and DTM expression under noninducing conditions, i.e., minus IPTG (data not shown). A low level of leakiness is a known feature of this particular expression system (Novagen, pET System Manual, 6th ed.).

Expression of a DTM-Associated Deoxyribonuclease Activity. After sample solubilization with Tergitol NP-40, a nondenaturing, nonionic detergent, electrophoresis of IPTG-induced *E. coli* in a DNA-embedded gel (Figure 4) shows that expression of the DTM protein (lane 3, CB-stained gel segment) is associated with expression of a comigrating nuclease-active band (lanes 5 and 7, EB-stained gel segment). Under nondenaturing conditions, the DTM protein (lane 3) runs faster than intact wild-type DTx protein (lane 1) because of its lower isoelectric point and lower molecular weight. The DTM-associated nuclease activity (lanes 5 and 7) also runs faster than intact DTx-associated nuclease activity (lane 8) under these conditions.

Samples in lanes 4 and 5 were solubilized for 5 min in Tergitol NP-40 (37 °C), whereas samples in lanes 6 and 7 were solubilized for 10 min in Tergitol NP-40 (37 °C). Longer solubilization times produced results similar to those seen in lanes 6 and 7. Samples of IPTG-treated *E. coli* that did not contain any toxin gene are shown in lane 2 (CB-stained gel) and lanes 4 and 6 (EB-stained gel). Under these sample conditions, an intrinsic *E. coli* nuclease activity (labeled Ec-nuc) is detected. It is located below the nuclease activity associated with the DTM protein band, or with the intact DTx band.

The DTM-Associated Deoxyribonuclease Activity Survives Electrophoresis under Denaturing Conditions. When *E. coli* carrying the plasmid without a toxin gene were treated with IPTG and electrophoresed under nonreducing conditions in a DNA-embedded SDS−polyacrylamide gel (Figure 5), we detected an endogenous *E. coli* nuclease (lane 7). In DTM-expressing *E. coli*, there are two distinct nuclease-active bands (lane 8). A comparison of the sample in lane 8 with the control sample in lane 7 demonstrates that the DTM nuclease has a higher molecular weight than the *E. coli* nuclease. The DTM-associated nuclease (lane 8) runs with a higher molecular weight than the CRM197 A domain-associated nuclease (lane 9), because the DTM protein contains a 23-amino acid extension at its carboxy terminus.

After the gel in Figure 5 was stained with EB for detection of nuclease activity (top panel), it was subsequently stained with CB (bottom panel). The R_f values for the CB-stained DTM and CRM197 A domain protein bands seen in lanes 8′ and 9′ are the same as the R_f values for the nuclease-active DTM and the nuclease-active CRM197 A domain bands seen in lanes 8 and 9, respectively. The endogenous *E. coli* nuclease is barely detectable under these conditions. We predicted that this was because the endogenous *E. coli* nuclease was present in much lower concentrations than the IPTG-induced DTM and therefore would more readily

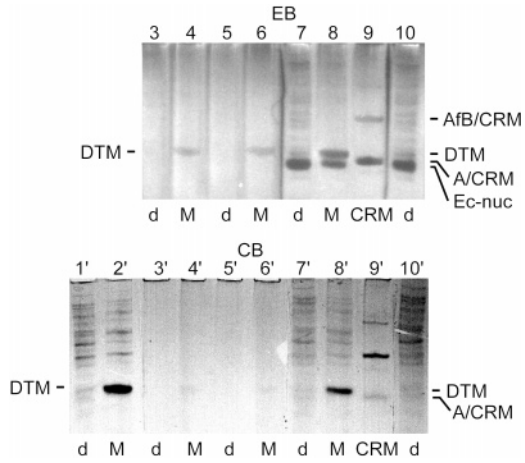

FIGURE 5: Nuclease activity of DTM after electrophoresis under denaturing, nonreducing conditions. Lanes 7 and 10 contain control *E. coli* (+ pET23-d), and lanes 3 and 5 contain $^1/_{10}$ and $^1/_{20}$ the amount of sample in control lanes 7 and 10. Lane 8 contains a sample of DTM-expressing *E. coli* (+ pET23-dM), and lanes 4 and 6 contain $^1/_{10}$ and $^1/_{20}$ the amount of sample in lane 8. Lane 9 contains argC-nicked CRM197 (1.15 μg). All *E. coli* samples were induced with IPTG. After electrophoresis, the gel was cut into three segments containing lanes 3−6, 7−9, and 10, respectively. These were separately tested for nuclease activity. The dark, nonfluorescent regions of the EB-stained gel represent areas of DNA degradation by underlying nuclease active proteins. After EB staining, lanes 3−10 were stained with CB as shown in lanes 3′−10′. Samples in lanes 1′ and 2′ are identical to samples shown in lanes 7′ and 8′, except that lanes 1′ and 2′ were CB-stained immediately after electrophoresis. Ec-nuc designates the position of an endogenous *E. coli* nuclease.

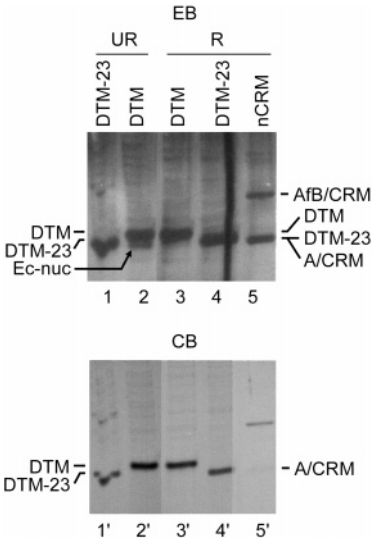

FIGURE 6: Nuclease activity of DTM and DTM-23 after electrophoresis under denaturing conditions. Lanes 1 and 4 contain DTM-23-expressing *E. coli* electrophoresed under nonreducing (UR) and reducing (R) conditions, respectively; lanes 2 and 3 contain DTM-expressing *E. coli* electrophoresed under nonreducing and reducing conditions, respectively; and lane 5 contains argC-nicked CRM197 (1.15 μg) under reducing conditions. All *E. coli* samples were induced with IPTG. Electrophoresis in a DNA-embedded SDS−polyacrylamide gel and subsequent gel treatments were as described (Experimental Procedures). The dark, nonfluorescent regions of the EB-stained gel represent areas of DNA degradation by underlying nuclease active proteins. After EB staining, lanes 1−5 were stained with CB as shown in lanes 1′−5′. Under nonreducing conditions, the endogenous *E. coli* nuclease (Ec-nuc) migrated with a lower molecular weight (arrow, lane 2).

renature, express activity, and leach out of the gel before it could be optimally visualized with CB. Lanes 1′ and 2′ are identical to lanes 7′ and 8′, except that lanes 1′ and 2′ were CB-stained immediately after electrophoresis (i.e., not subjected to lengthy treatments for expression of nuclease activity). As predicted, the protein band corresponding to the position of the *E. coli* nuclease and that corresponding to the position of the DTM nuclease are both more readily detectable in the gel lanes that were stained with CB immediately (lanes 1′ and 2′). The control sample in lane 10 is identical to that in lane 7. However, immediately after electrophoresis, lane 10 was cut from the rest of the gel and treated separately throughout so as to demonstrate the reproducibility of the procedure for detecting nuclease activity.

Less sample was run in lanes 3−6 to determine whether DTM or the endogenous *E. coli* nuclease was the first to be detected. Lanes 3 and 5 contain $^1/_{10}$ and $^1/_{20}$ less sample than lane 7, and lanes 4 and 6 contain $^1/_{10}$ and $^1/_{20}$ less sample than lane 8. These four lanes were treated similarly to lanes 7 and 8, except that they were incubated with divalent cations for a longer time before staining with EB. As shown, DTM's nuclease activity was readily detected in lanes 4 and 6, but at a lower intensity than in lane 8. After staining the gel with CB, two faint protein bands appeared in lanes 4′ and 6′, proteins that correspond in position to the DTM nuclease-active bands seen in lanes 4 and 6. At these low sample concentrations, no intrinsic *E. coli* nuclease activity was detected in the control samples (lanes 3 and 5). Thus, expression of nuclease activity at the band position of DTM and at these low sample concentrations is only possible when *E. coli* carries and expresses the gene for DTM.

The nuclease-active band labeled AfB/CRM in lane 9 was identified by amino acid sequencing and Western blot analysis as the entire A domain of CRM197 plus a covalently attached fragment of the B domain. The dark band in lane 9′ is protein-stained AfB/CRM. The apparent molecular mass of this nuclease-active CRM197 fragment is 40 kDa.

The Deoxyribonuclease Activity of E. coli-Cloned DTM and DTM-23. In Figure 6, gel lanes 1−5 were EB-stained to detect nuclease activity and then CB-stained to pinpoint protein locations (lanes 1′−5′). The results show that nuclease activity comigrates with DTM (lanes 2 and 3) and with DTM-23 (lanes 1 and 4) under both nonreducing, denaturing (lanes 1 and 2) and reducing, denaturing conditions (lanes 3 and 4). Significantly, removal of DTM's 23-amino acid carboxy-terminal extension resulted in expression of a protein (DTM-23) that migrated with a lower molecular weight than DTM. This is evident when CB-stained lanes 1′ and 4′ are compared with lanes 2′ and 3′. The lower molecular weight DTM-23 protein was also able to renature and express nuclease activity (lanes 1 and 4) similar in potency to that of DTM (lanes 2 and 3). The fact that reduced DTM did not migrate with the same molecular weight as DTM-23 means that the *E. coli*-expressed DTM was not cleaved between its A domain and its 23-amino acid extension. If it had been cleaved, reduction would have resulted in the loss of the extension, and then DTM would have migrated to the same gel position as both DTM-23 and the A domain of endoproteinase argC-nicked CRM197 (lane 5). The data also indicate that the presence of the randomly generated 23-amino acid extension on DTM does not affect its ability to renature and express nuclease activity in this gel system.

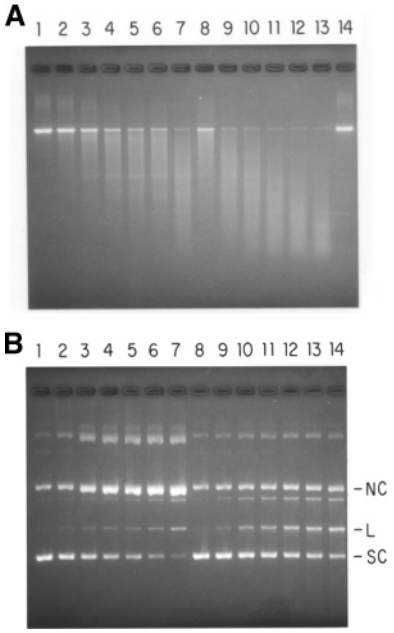

FIGURE 7: Divalent cations regulate the mechanism of endonucleolytic cleavage by CRM197. (A) CRM197 (0.044 μg) and linearized pUC8 DNA (0.12 μg) were incubated for 1, 2, 3, 4, 5, and 6 min in buffer containing either 2 mM Ca^{2+} plus 3 mM Mg^{2+} (lanes 2−7) or 10 mM Mn^{2+} alone (lanes 8−13). Lane 1 contains DNA in Ca^{2+}/Mg^{2+} buffer and lane 14 contains DNA in Mn^{2+} buffer, without protein. (B) Samples in lanes 1−7 contain Ca^{2+} plus Mg^{2+}. Samples in lanes 8−14 contain Mn^{2+}. Samples in lanes 1 and 8 were incubated without CRM197. Those in lanes 2−7 and in lanes 9−14 were incubated with CRM197 (0.011 μg) for 1, 3, 5, 7, 10, and 15 min, respectively. *Sc* represents supercoiled DNA, *nc* represents nicked circular DNA, and *l* represents linearized DNA. For details see Experimental Procedures.

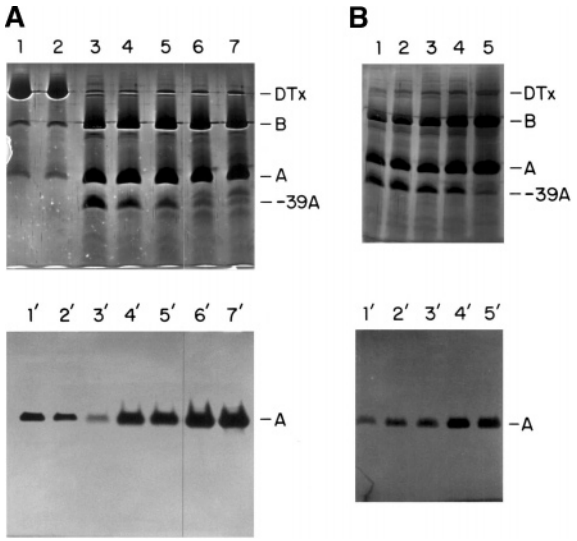

FIGURE 8: DNA and NAD protect the A domain of DTx from enzymic cleavage. (A) Lane 1 contains "intact" DTx that was incubated with 10 μg of λDNA in the absence of trypsin. Lane 2 contains "intact" DTx that was incubated without λDNA in the absence of trypsin. Lanes 3−7 contain "intact" DTx after treatment with trypsin in the presence of 0, 0.1, 1.0, 5.0, and 10 μg of λDNA, respectively. (B) Lanes 1−5 contain "intact" DTx after treatment with trypsin in the presence of 0, 0.1, 1.0, 5.0, and 10 μg of NAD, respectively. (Top panels) Silver-stained protein samples after SDS−polyacrylamide gel electrophoresis under reducing conditions. (Bottom panels) Identically prepared samples after electrophoresis in a DNA-containing SDS−polyacrylamide gels under reducing conditions. Here the gels were washed and incubated for expression of nuclease activity as described (Experimental Procedures) and then stained with EB.

Lanes 2′ and 3′ show that DTM's gel position does not change upon reduction. A comparison of lanes 2 and 3 shows that the *E. coli* nuclease-active band (Ec-nuc) is not separable from DTM's nuclease activity under reducing conditions. An independent comparison of reduced and nonreduced *E. coli* control samples confirmed that, under reducing conditions, Ec-nuc moves slightly slower in SDS gels and retains nuclease activity (data not shown). Lane 2 shows that under nonreducing conditions, Ec-nuc shifts downward to a position that is clearly distinguishable from that of the DTM nuclease-active band. This finding is a confirmation of the result shown in Figure 5, lane 8.

The nuclease active-band labeled AfB/CRM in Figure 6, lane 5, provides confirmation of the result shown in Figure 5, lane 9, i.e., that a 40-kDa protein consisting of the entire A domain of CRM197 plus a covalently attached fragment of the B domain can renature and express nuclease activity.

Divalent Cations Regulate the Mechanism of Endonucleolytic Cleavage by CRM197. When the ADPrT-defective CRM197 was combined with linear dsDNA in buffer containing either 2 mM Ca^{2+} plus 3 mM Mg^{2+} or 10 mM Mn^{2+} alone, significant nuclease activity was observed. Figure 7A shows the reaction products generated after 1−6 min at 37 °C. DNA degradation was rapid and extensive under both sets of conditions, but in the presence of Mn^{2+}, the substrate material was degraded at a much faster rate. Figure 7B shows the results obtained when supercoiled dsDNA (*sc*) was incubated with CRM197 at 22 °C for defined times in buffer containing either 2 mM Ca^{2+} plus 3 mM Mg^{2+} (lanes 2−7) or 10 mM Mn^{2+} alone (lanes 9−14). Reaction conditions were chosen to allow for detection of initial reaction products. In the presence of Ca^{2+} plus Mg^{2+}, CRM197 led to the sequential appearance of nicked-circular DNA (*nc*) and then linear DNA (*l*). This pattern indicates that cleavage in the presence of Ca^{2+} plus Mg^{2+} leads to the accumulation of single-strand nicks. In the presence of Mn^{2+}, CRM197 led directly to the accumulation of unit-sized linear DNA without a similar increase in nicked-circular intermediates. Similar results were obtained with DTx.[4] Thus, the mechanism of DNA cleavage by both DTx and CRM197 shifts to the generation of double-strand breaks in the presence of Mn^{2+}.

DNA Protects the Nuclease Activities of the A Domains of DTx and CRM197. When "intact" DTx was incubated without trypsin in the presence (Figure 8A, lane 1) or absence (Figure 8A, lane 2) of 10 μg of λDNA, the low levels of free A domain in these "intact" DTx samples, an amount requiring silver staining to detect (top panel), exhibited significant nuclease activity (bottom panel) in a gel embedded with calf thymus DNA. When "intact" DTx was incubated with trypsin in the absence of λDNA, the DTx was cleaved into its B and A domains (lane 3, top panel). The A domain exhibited nuclease activity (lane 3′, bottom panel). However, some of the A domain was further cleaved to a protein designated −39A (lane 3, top panel). Sequencing revealed that this cleavage product lacked 39 amino-terminus amino acids. Under these assay conditions, protein −39A exhibited no nuclease activity (lane 3′, bottom panel). When "intact" DTx was incubated with trypsin plus increasing amounts of

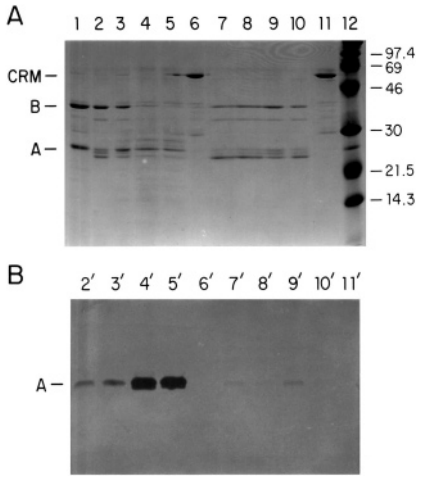

FIGURE 9: DNA (but not NAD) protects the A domain of CRM197 from enzymic cleavage. Lane 1 contains argC-nicked CRM197; lanes 2−5 contain "intact" CRM197 after treatment with trypsin in the presence of 0, 0.1, 5.0, and 10 μg of λDNA, respectively; lane 6 contains "intact" CRM197 that was incubated with 10 μg of λDNA in the absence of trypsin. Lanes 7−10 contain "intact" CRM197 after treatment with trypsin in the presence of 0, 0.1, 5.0, and 10 μg of NAD, respectively; lane 11 contains "intact" CRM197 that was incubated with 10 μg of NAD in the absence of trypsin. Lane 12 contains molecular weight markers. (A) Lanes 1−12 are CB-stained samples after SDS−polyacrylamide gel electrophoresis under reducing conditions. (B) Lanes 2′−11′ are identical to reduced samples 2−11 in panel A except that electrophoresis was performed in a DNA-embedded SDS−polyacrylamide gel that was subsequently washed and incubated for expression of nuclease activity as described (Experimental Procedures) and then stained with EB.

λDNA (0.1, 1.0, 5.0, and 10 μg), the λDNA dramatically protected the A domain from trypsin cleavage (lanes 4−7, top panel) and from concomitant destruction of the A domain's nuclease activity (lanes 4′−7′, bottom panel).

Data in Figure 9 show that increasing amounts of λDNA (0, 0.1, 5.0, and 10 μg) likewise protected the A subunit of CRM197 from trypsin cleavage (lanes 2−5, top panel) and from loss of nuclease activity (lanes 2′−5′, bottom panel). Lane 1 contains an endopeptidase argC-cleaved sample of CRM197 to pinpoint the A and B domains. Figure 9 also shows a sample of "intact" CRM197 that was incubated without trypsin in the presence of 10 μg of λDNA. No detectable free A domain is seen in this "intact" CRM197 preparation (lane 6, top panel), nor is any nuclease activity observed at the A domain band position (lane 6′, bottom panel). Thus, detection of nuclease activity in this assay system is dependent on the presence and intactness of the A domains of both DTx and CRM197.

NAD Protects the Nuclease Activity of the A Domain of DTx but Not That of CRM197. Data in Figure 8B show that increasing amounts of NAD (0, 0.1, 1.0, 5.0, and 10 μg) protect the A domain of DTx from trypsin cleavage (lanes 1−5, top panel) and from concomitant destruction of A-domain-associated nuclease activity (lanes 1′−5′, bottom panel). Significantly, data shown in Figure 9 establish that increasing amounts of NAD (0, 0.1, 5.0, and 10 μg) do not protect the A domain of CRM197 from trypsin cleavage (lanes 7−10, top panel) or from concomitant destruction of the A domain's nuclease activity (lanes 7′−10′, bottom panel). Lane 11 in Figure 9 shows a sample of "intact" CRM197 that was incubated without trypsin in the presence of 10 μg of NAD. Neither free A domain protein nor any nuclease activity is detectable in this "intact" CRM197 sample.

Protection results similar to those in Figures 8 and 9 were obtained when we started with endopeptidase argC-cleaved DTx and CRM197 preparations (data not shown). Conditions were such that precleavage of the proteins into whole A and B domains was complete within 1 h, with no further cleavage being noted after longer incubations. Thus, any cleavage of the A domains that occurred in the subsequent DNA and NAD protection assays could be attributed to the presence of trypsin.

DISCUSSION

The cytotoxic mechanism of DTx has long been accepted to be dependent upon the ability of its A domain to inhibit protein synthesis by NAD-dependent ADP-ribosylation of the diphthamide residue of EF-2 (*19*−*21*). However, we and others have demonstrated that there is no correlation between cell lysis and protein synthesis inhibition as effected by a number of toxins and treatments (*1*, *2*). This lack of correlation led to the discoveries that DTx induces internucleosomal DNA cleavage in target cells and that endonucleolytic degradation of DNA is an intrinsic enzymic activity of the toxin's A domain (*1*, *3*, *4*). Subsequently, we discovered that the A domain of CRM197, a well-characterized ADPrT-deficient form of DTx, also possesses nuclease activity and that its specific activity is 4 times greater than that of bovine pancreatic DNase I and 20 times greater than that of DTx (*3*, *13*).

Although the DTM mutant form of the A domain of DTx was selected for its temperature-dependent growth effects in yeast, it fortuitously turned out to possess the same point mutation as the A domain of CRM197 (*15*). Our studies of *E. coli*-cloned DTM and the related protein DTM-23 show that deoxyribonuclease activity comigrates with these two proteins under conditions in which they run with distinctive molecular weights (in denaturing gels) and distinctive charge properties (in nondenaturing gels). Similar nuclease results were obtained with *E. coli*-cloned forms of the A domain of DTx, DTA, and DTA-23,[4] proteins that are distinguishable from each other and from DTM and DTM-23 under both denaturing and nondenaturing gel conditions (Figure 3). To rule out the possibility that DTM might fold into an active ADPrT at low temperatures and thereby mediate ADPrT-induced toxic effects when expressed in yeast and *Drosophila*, we produced mutant A domain proteins by in vitro transcription/translation and assessed their relative abilities to ADP-ribosylate EF-2. The results establish that DTM lacks the ability to ADP-ribosylate EF-2 (Figure 2) or shut off protein synthesis[2,4] at both 18 and 30 °C. This agrees with data showing that CRM197 lacks ADPrT activity between 0 and 37 °C,[2,3] while its nuclease activity retains the same temperature dependency as DTx (*7*).

We have demonstrated herein that despite amino- and carboxy-terminal differences between DTM and the A chain of CRM197 (Figure 1), DTM retains the ability to degrade DNA. Hence, a possible explanation for the observation (*15*) that DTM-expressing yeast exhibit growth inhibition at 18 °C and grow normally at 30 °C is greater induction of DNA-damage-inducible genes at 30 °C. When this hypothesis was tested, we found that galactose induction of the DTM gene

in yeast caused transcription of two distinct families of DNA-damage-response genes (*22*).[2] Wild-type-like growth at 30 °C was correlated with very high levels of transcription of these DNA-damage-response genes. In contrast, DTM expression at 18 °C resulted in significantly lower levels of repair-enzyme induction. We also found[4] that after 96 h, neither the DTM-mediated effects on yeast at 18 °C nor the DTA-mediated effects at 18 and 30 °C were due to cell death but rather to fully reversible growth inhibition, emphasizing once again that protein synthesis inhibition and cell death are not directly correlated. The simplest answer to why expression of the cloned wild-type A domain (DTA) leads to growth inhibition at both 18 and 30 °C is that this protein possesses the additional ability to inhibit the synthesis of needed DNA repair enzymes. We conclude that insufficient induction and/or synthesis of repair enzymes creates a situation in which DNA damage mediated by the nuclease activity of DTM at 18 °C and of DTA at 18 and 30 °C overwhelms the repair capacity of the cells. This in turn leads to a state of reversible mitotic arrest.

It should be noted that no cytotoxic effects have been reported upon extracellular addition of CRM197 to mammalian cell targets. However, no study has ever tested the ability of the A domain of CRM197 to traverse the membrane bilayer. In addition, Bellen et al. have shown that the A domain equivalent of CRM197, i.e., DTM, only exhibits cytotoxic effects at low temperatures and, to date, no studies have been done to test whether a several-hour drop to 16−18 °C would lead to CRM197-specific cytotoxic effects in mammalian cell targets as they did with yeast and *Drosophila* (*15*). More studies are needed before it can be concluded that CRM197 has no effect on typical target cells.

Because our results indicate that DTM and CRM197 are functionally identical, i.e., share an ability to degrade DNA (Figures 5 and 6) at a rate higher than that of DTA or DTx (data not shown; ref *13*) and lack ADPrT activity at 18 and 30 °C (Figure 2),[2,3] we proceeded to utilize the more readily available CRM197 in subsequent characterization assays. We found that for both CRM197 and DTx, Ca^{2+} and Mg^{2+} promote single-strand nicks, whereas Mn^{2+} promotes double-strand breaks (Figure 7B).[4] These findings are similar to X-ray findings with bovine pancreatic DNase I:DNA co-crystals (*23*). With ssDNA, Mn^{2+} leads to no increase in cleavage rate over that seen with Ca^{2+} and Mg^{2+} (data not shown). Our protection assays further establish (1) that DNA protects the A domains of both DTx and CRM197 from trypsin cleavage, (2) that NAD only protects the A domain of DTx from trypsin cleavage, and (3) that the protected A domains are required for expression of nuclease activity. These results demonstrate that the A domains of both DTx and CRM197 have the ability to bind DNA and that the A domain of CRM197 lacks the ability to bind NAD. Because the addition of Ca^{2+} and Mg^{2+} to the trypsin cleavage studies of DTx and CRM197 abolished the protection by λDNA and permitted the λDNA to be cleaved (as observed by λDNA digestion products below the sample wells; data not shown), we conclude that avid binding of DNA to both the A domains of DTx and CRM197 does not require divalent cations. These and other data show that trypsin activity is not affected by the presence of DNA.

There is substantial evidence that DTx possesses nuclease activity and that this activity is independent of its ADPrT activity. Examples are (i) X-ray crystal-grade CRM45, a form of DTx with a foreshortened carboxy-terminus B domain, and its A domain possess nuclease activity (*9*); (ii) all protein-containing samples provided by R. J. Collier (Harvard Medical School), including a sample of FPLC-purified *E. coli*-cloned wild-type A domain and the ADPrT-deficient E148S mutant form of DTx, likewise exhibit nuclease activity (*4*); (iii) the A domains of both DTx and the ADPrT-deficient CRM197 as well as cloned forms of these A domains (DTA, DTA-23, DTM, and DTM-23) all possess nuclease activity (data herein);[4] (iv) the pH and temperature optima of the A domain's nuclease activity (7.4 and 37 °C, respectively (*7*)) and ADPrT activity (8.5 and 25 °C, respectively (*5*, *20*)) are distinct; (v) competitive inhibitors of the ADPrT activity of DTx, e.g., NAD, ATP, adenine, nicotinamide and ApUp, have no competitive effect on the nuclease activity of DTx (*24*); (vi) DNA does not inhibit the ADPrT activity of DTx (*24*); (vii) DNA binds to the A domains of both DTx and CRM197 and protects the same sequence-defined sites from proteolytic cleavage, whereas NAD protects only the A domain of DTx from proteolytic cleavage, at unique sites (Figures 8 and 9);[4] (viii) divalent cations have no effect on the ADPrT activity of DTx (*6*) but are necessary for nuclease activity (*3*, *7*); (ix) nuclease activity does not require toxin cleavage and reduction to separate the A domain from the B domain of DTx (*3*, *8*, *9*) but ADPrT activity does (*6*); and (x) site-specific antibodies targeting residues 32−54, a portion of the DTx sequence responsible for ADPrT activity, inhibit ADPrT activity by 86.2% without a corresponding drop in cell death (*25*).

Several lines of evidence suggest that DTx may not be alone in its ability to shut off protein synthesis and alter DNA. For example, the carboxy-terminal enzymic domain of *Pseudomonas exotoxin* A, which contains sequence and structural homologies to the amino-terminal enzymic A domain of DTx (*26*, *27*), was shown to possess an ability to degrade DNA (*28*) in addition to its DTx-like ability to inhibit protein synthesis by ADP-ribosylating the diphthamide residue of EF-2. Having shown that the antitumor, antiviral, and antiparasitic effects of ribosome-inactivating proteins such as gelonin and pokeweed antiviral protein are not solely due to ribosome inactivation (*29*−*32*), searches for alternative substrates revealed that these proteins also possess an ability to remove adenines from ssDNA (*33*). Thus, Taraschi and co-workers concluded that if the number of DNA breaks resulting from the removal of closely spaced adenine residues overwhelmed the DNA repair capacity of the cell or organism, the adenine glycosylase activity of the ribosome-inactivating proteins could be mutagenic or lethal (*34*). Interestingly, Collier suggested that DTx may have evolved from a nucleic acid-binding protein (*6*). In this regard, Figure 10 shows significant sequence homologies between the A domain of DTx and four well-characterized nucleases, namely, yeast nuclear endo-exonuclease, yeast mitochondrial endonuclease, *Neurospora crassa* endonuclease, and a nuclease encoded by the herpes simplex type 1 virus (Fraser, M.J. Personal communication; refs *35*−*37*).[5]

In the light of the lack of correlation between DTx's protein synthesis inhibition activity and cell death (*1*) and the ADPrT-deficient DTM's ability to cause both apoptosis

[5] M. J. Fraser, personal communication.

FIGURE 10: Sequence homologies between the A domain of DTx (DTx A) and four well-characterized nucleases: yeast nuclear endo-exonuclease (Y Nuc), yeast mitochondrial endonuclease (Y Mito), *Neurospora crassa* endonuclease (Nc Nuc), and a nuclease encoded by the herpes simplex type 1 virus (HSV Nuc). Symbols: ■, identity; ●, highly conserved; ○, chemical similarity (data provided by M. J. Fraser).

of *Drosophila* photoreceptor cells and inhibition of yeast growth, we propose that it is the nuclease activity of the wild-type A domain that is the main contributor to the toxin's cytotoxicity. The findings described herein lend strong support to the notion that DTx "acts as a double-edged sword using apparently nonoverlapping sites to effect translation inhibition and chromosomal cleavage" (*13*). Indeed, the combination of these abilities gives DTx the advantage of being able to effect internucleosomal DNA degradation while simultaneously shutting off the synthesis of the very proteins needed to repair it.

Future studies will focus on the production of nuclease-deficient forms of the A domain of DTx that retain ADPrT activity. Having defined by sequencing the regions of the A domains of DTx and CRM197 that are uniquely protected from proteolytic cleavage in the presence of DNA (versus NAD)[4] should aid in the construction of nuclease-inactive, ADPrT-active proteins. Such proteins would enable us to delineate the respective roles of these two distinct enzymic activities.

ACKNOWLEDGMENT

We thank Dr. Hugo Bellen for supplying plasmids bearing the genes for DTA and DTM, Dr. Mark Stolowitz for sequencing the trypsin-generated peptides of DTx and CRM197, and Louis Chau, Joshua Fleishman, Lawrence Nakamura, Christine Spector, and Rong Yang for expert technical support.

REFERENCES

1. Chang, M. P., Bramhall, J., Graves, S., Bonavida, B., and Wisnieski, B. J. (1989) Internucleosomal DNA cleavage precedes diphtheria toxin induced cytolysis-Evidence that cell lysis is not a simple consequence of translation inhibition, *J. Biol. Chem. 264*, 15261−15267.
2. Sung, C., Wilson, D., and Youle, R. J. (1991) Comparison of protein-synthesis inhibition-Kinetics and cell killing induced by immunotoxins, *J. Biol. Chem. 266*, 14159−14162.
3. Chang, M. P., Baldwin, R. L., Bruce, C., and Wisnieski, B. J. (1989) Second cytotoxic pathway of diphtheria toxin suggested by nuclease activity, *Science 246*, 1165−1168.
4. Lessnick, S. L., Lyczak, J. B., Bruce, C., Lewis, D. G., Kim, P. S., Stolowitz, M. L., Hood, L., and Wisnieski, B. J. (1992) Localization of diphtheria-toxin nuclease activity to fragment A, *J. Bacteriol. 174*, 2032−2038.
5. Collier, R. J., and Kandel, J. (1971) Structure and activity of diphtheria toxin. I. Thiol-dependent dissociation of a fraction of toxin into enzymically active and inactive fragments, *J. Biol. Chem. 246*, 1496−1503.
6. Collier, R. J. (1982) in *ADP−Ribosylation Reactions* (Hayaishi, O., and Ueda, K., Eds) pp 575−592, Academic Press, Orlando, FL.
7. Nakamura, L. T., and Wisnieski, B. J. (1990) Characterization of the deoxyribonuclease activity of diphtheria toxin, *J. Biol. Chem. 265*, 5237−5241.
8. Lessnick, S. L., Bruce, C., Baldwin, R. L., Chang, M. P., Nakamura, L. T., and Wisnieski, B. J. (1990) Does diphtheria toxin have nuclease activity?—Reply, *Science 250*, 832−838.
9. Wisnieski, B. J., Amini, S. M., and Tseng, Y. (1998) Characterization of the deoxyribonuclease and ADP-ribosyltransferase activities of CRM45, a truncated homologue of diphtheria toxin, *J. Natural Toxins 7*, 255−267.
10. Uchida, T., Pappenheimer, A. M., Jr., and Greany, R. (1973) Diphtheria toxin and related proteins. I. Isolation and properties of mutant proteins serologically related to diphtheria toxin, *J. Biol. Chem. 248*, 3838−3844.
11. Lory, S., Carroll, S. F., and Collier, R. J. (1980) Ligand interactions of diphtheria toxin. II. Relationships between the NAD site and the P site, *J. Biol. Chem. 255*, 12016−12019.
12. Uchida, T., Pappenheimer, A. M., Jr., and Harper, A. A. (1972) Reconstitution of diphtheria toxin from two nontoxic cross-reacting mutant proteins, *Science 175*, 901−903.
13. Bruce, C., Baldwin, R. L., Lessnick, S. L., and Wisnieski, B. J. (1990) Diphtheria-toxin and its ADP-ribosyltransferase-defective homologue CRM197 possess deoxyribonuclease activity, *Proc. Natl. Acad. Sci. U.S.A. 87*, 2995−2998.
14. Yamaizumi, M., Uchida, T., Takamatsu, K., and Okada, Y. (1982) Intracellular stability of diphtheria toxin fragment A in the presence and absence of anti-fragment A antibody, *Proc. Natl. Acad. Sci. U.S.A. 79*, 461−465.
15. Bellen, H. J., D'Evelyn, D., Harvey, M., and Elledge, S. J. (1992) Isolation of temperature sensitive diphtheria toxins in yeast and their effects on Drosophila cells, *Development 114*, 787−796.
16. Laemmli, U. K. (1970) Cleavage of structural proteins during the assembly of the head of bacteriophage T4, *Nature 227*, 680−685.
17. Rosenthal, A. L., and Lacks, S. A. (1977) Nuclease detection in SDS-polyacrylamide gel electrophoresis, *Anal. Biochem. 80*, 76−90.
18. Maxwell, F., Maxwell, I. H., and Glode, L. M. (1987) Cloning, sequence determination, and expression in transfected cells of the coding sequence for the tox 176 attenuated diphtheria toxin A chain, *Mol. Cell Biol. 7*, 1576−1579.
19. Honjo, T., Nishizuka, Y., Hayaishi, U., and Kato, J. (1968) Diphtheria toxin-dependent adenosine diphosphate ribosylation of aminoacyl transferase II and inhibition of protein synthesis, *J. Biol. Chem. 243*, 3553−3555.
20. Collier, R. J. (1975) Diphtheria toxin: Mode of action and structure, *Bacteriol. Rev. 39*, 54−85.
21. Pappenheimer, A. M., Jr. (1977) Diphtheria toxin, *Annu. Rev. Biochem. 46*, 69−94.
22. Shi, D. P., Sodhi, A., Gordon, R., and Wisnieski, B. J. (1995) Intracellular expression of the A chains of diphtheria toxin and CRM 197 are associated with DNA repair enzyme expression and cell cycle arrest in yeast. *Abstracts of the 95th General Meeting of the American Society for Microbiology*, p 234.
23. Suck, D., Lahm, A., and Oefner, C. (1988) Structure refined to 2Å of a nicked DNA octanucleotide complex with DNase I, *Nature 332*, 464−468.
24. Lee, J. W., Nakamura, L. T., Chang, M. P., and Wisnieski, B. J. (2004) Mechanistic aspects of the deoxyribonuclease activity of diphtheria toxin, *Biochim. Biophys. Acta*. In press.
25. Olson, J. C. (1993) Use of synthetic peptides and site-specific antibodies to localize a diphtheria toxin sequence associated with ADP-ribosyltransferase activity, *J. Bacteriol. 175*, 898−901.
26. Allured, V. S., Collier, R. J., Carroll, S. F., and McKay, D. B. (1986) Structure of exotoxin A of *Pseudomonas aeruginosa* at 3.0 Å resolution, *Proc. Natl. Acad. Sci. U.S.A. 83*, 1320−1324.
27. Choe, S., Bennett, M. J., Fujii, G., Curmi, P. M. G., Kantardjieff, K. A., Collier, R. J., and Eisenberg, D. (1992) The crystal structure of diphtheria toxin, *Nature 357*, 216−222.
28. Bruce, C. (1990) Ph.D. Thesis, University of California, Los Angeles.
29. Teltow, G. J., Irvin, J. D., and Aron, G. M. (1983) Inhibition of herpes simplex virus DNA synthesis by pokeweed antiviral protein, *Antimicrob. Agents Chemother. 23*, 390−396.
30. McGrath, M. S., Hwang, K. M., Caldwell, S. E., Gaston, I., Luk, K.-C., Wu, P., Ng, V. L., Crowe, S., Daniels, J., Marsh, J., Deinhart, T., Lekas, P. V., Vennari, J. C., Yeung, H.-W., and Lifson, J. D. (1989) GLQ223: An inhibitor of human immunodeficiency virus replication in acutely and chronically infected cells of lymphocyte and mononuclear phagocyte lineage, *Proc. Natl. Acad. Sci. U.S.A. 86*, 2844−2848.
31. Tumer, N. E., Hwang, D.-J., and Bonness, M. (1997) C-terminal deletion mutant of pokeweed antiviral protein inhibits viral infection but does not depurinate host ribosomes, *Proc. Natl. Acad. Sci. U.S.A. 94*, 3866−3871.
32. Nicolas, E., Goodyer, I. D., and Taraschi, T. F. (1997) An additional mechanism of ribosome-inactivating protein cytotoxicity: Degradation of extrachromosomal DNA, *Biochem. J. 327*, 413−417.
33. Nicolas, E., Beggs, J. M., Haltiwanger, B. M., and Taraschi, T. F. (1998) A newclass of DNA glycosylase/apurinic/apyrimidinic lyases that act on specific adenines in single-stranded DNA, *J. Biol. Chem. 273*, 17216−17220.

34. Nicolas, E., Beggs, J. M., and Taraschi, T. F. (2000) Gelonin is an unusual DNA glycosylase that removes adenine from single-stranded DNA, normal base pairs and mismatches, *J. Biol. Chem. 275*, 31399−31406.

35. Fraser, M. J., Koa, H., and Chow, T. Y. K. (1990) Neurospora endo-exonuclease is immunochemically related to the recC gene product of *Escherichia coli*, *J. Bacteriol. 172*, 507−510.

36. Fraser, M. J., Hatahet, Z., and Huang, X. (1989) The actions of Neurospora endo-exonuclease on double strand DNAs, *J. Biol. Chem. 264*, 13093−13101.

37. Knopf, C. W., and Weisshart, K. (1990) Comparison of exonucleolytic activities of herpes simplex virus type-1 DNA polymerase and DNase, *Euro J. Biochem. 191*, 263−273.

BI048317P